Contribution of FACTS Devices to the Transient Stability Improvement of a Power System Integrated with a PMSG-Based Wind Turbine

Nice Enyonam Akpeke
Department of Electrical Engineering, PAU Institute for Basic Sciences Technology and Innovation, Nairobi, Kenya
niceenyonam@gmail.com

Cristopher Maina Muriithi
Department of Electrical Engineering, Murang'a University of Technology, Murang'a, Kenya
cmainamuriithi@gmail.com

Charles Mwaniki
School of Engineering and Technology, Machakos University, Machakos, Kenya
cmwaniki@mksu.ac.ke

***Abstract*—The increasing penetration of wind energy to the conventional power system due to the rapid growth of energy demand has led to the consideration of different wind turbine generator technologies. In fault conditions, the frequency of the power system decreases and eventually leads to speed differences between the grid and the interconnected wind generator. This can result to power system problems such as transient instability (TS). This paper focuses on enhancing the TS of a permanent magnet synchronous generator (PMSG)-based power system during 3ph fault conditions using FACTS devices. The power system considered is connected to a large wind farm which is based on PMSG. Critical clearing time (CCT) is used as an index to evaluate the transient state of the system. Under the study of an IEEE-14 bus system using PSAT as a simulation tool, the integrated CCT with PMSG-based wind turbine is improved with three independent FACTS devices. One of the synchronous generators in the test system has been replaced at random with the PMSG-based wind turbine which is meant to generate an equivalent power. Time domain simulations (TDSs) were carried out considering four study cases. Simulation results show that the (CCT) of the system with the FACTS devices is longer than the CCT without them, which is an indication of TS improvement.**

Keywords-critical clearing time; FACTS; generator; transient statbility; wind

I. INTRODUCTION

Among renewable power sources, wind has been noted to be the fastest growing one to its clear and numerous advantages [1]. Transient stability (TS) which is the tendency of synchronous generators remaining in synchronism following a severe disturbance [1-4], is one of the major aspects of a power system that gets affected with the integration of large wind turbines. Globally, Squirrel Cage Induction Generator (SCIG), Doubly Fed Induction Generator (DFIG), and Permanent Magnet Synchronous Generator (PMSG) are common wind generator technologies considered in wind energy conversion. Unlike DFIG, the PMSG has a full-scale power converter [5]. It enables more reliable operation of wind turbines and reduces the required maintenance [6]. These features make PMSG more advantageous than DFIG. Currently, most wind energy conversion technologies employ turbines with PMSG [7, 8]. Even though the PMSG has a better reactive power capability, it is still not adequate as the principal precaution during transient conditions [9-10]. There is therefore a need to augment the dynamic reactive power capability of FACTS devices in order to strengthen the transient state of the system to which it is connected.

TS is considered one of power system's dynamic behaviors having been analyzed and improved by various approaches. However, since TS study can only be considered in the presence of a severe fault [4], there is need to mention the clearing time of faults which will keep the system transiently stable. For a particular given system, the critical clearing time (CCT) must be specified or stated to allow easy system operation during faults. In addition, TS study time is short and so faults need to be cleared as quickly as possible to prevent synchronism loss of the system generators, knowing the CCT can allow fault clearing within the time limit thereby maintaining the stability of the system. An impact study for PMSG-based wind generation on the TS was carried out in [7]. The study considered a method of equal area criteria theory. An active current control strategy taking into account a perturbation estimation was proposed in [11] for enhancing the TS of a power system connected with a PMSG-based turbine. A simulation study was conducted in [12] by using a TSSC to improve the efficiency of a wind turbine. Authors in [8] compared the TS augmentation between doubly fed induction generators and permanent magnet synchronous generators. It was deduced that the TS of the system with DFIG wind generator can be improved by including a permanent magnet synchronous generator in the same system. Authors in [13] investigated the effects of series compensation on the TS improvement for a DFIG wind turbine power system. In [14], a study of the assessment of wind energy based on SCIG penetration effect on TS was provided. Different penetration levels were considered and CCT was analyzed.

The current paper focuses on the TS analysis with consideration of critical clearing time index. Thus, conclusions on the improvement of the TS of the system are based on the CCTs of all the cases considered.

Corresponding author: Nice Enyonam Akpeke

II. IMPLEMENTATION OF THE SYSTEM IN PSAT

This paper employed the IEEE-14 bus system for the simulation process. Power System Analysis Toolbox (PSAT) was used in implementing the considered system. PSAT is a MATLAB package which uses Simulink libraries for network designs. It is appropriate for analysis of small and medium size power systems [15]. PSAT also supports both dynamic and static power system analysis and control studies. Aside time domain simulations, PSAT also includes optimal power flow, continuation power flow and small signal analysis. The data used in implementing the system in PSAT are taken from [16] with 20s simulation time.

A. The IEEE 14-bus System Model

The implementation of the proposed test system is executed using PSAT 2.1.10. Synchronous generator models, wind turbine model, wind turbine generator model, constant loads, and FACTS devices are all inherent models adopted from MATLAB/Simulink library. The test system consists of 5 generator buses and 8 load buses. Out of the 5 generator buses, there is one slack (bus 1), one PV (bus 2) and 3 additional synchronous condensers (buses 3, 6, 8). Table I shows a summary of the system characteristics.

TABLE I. MODIFIED IEEE-14 BUS, 5-MACHINE TEST SYSTEM

Equipment	Quantity
Buses	14
Generators	5
Transformers	4
Transmission lines	16
Loads	11

Three different voltage levels were chosen for the whole system equipment with a power rating of 100MVA. Blue indicates a 13.8kV bus, green indicates an 18kV bus and red indicates a 69kV bus. Bus 1 is defined to be the reference bus (where the wind turbine is integrated). The purpose of integrating the wind at the slack is to allow the wind turbine generate a greater percentage of the whole system capacity.

B. Modeling of the PMSG-based Turbine

The PMSG, also referred to as direct drive synchronous generator (DDSG), is a type of synchronous generator whose rotor windings are replaced with a permanent magnet and hence the name permanent magnet synchronous generator (PMSG). Its excitation field is created by the permanent magnet in the rotor [10]. This arrangement has led to the elimination of excitation losses that will take place in the rotor during starting of the generator.

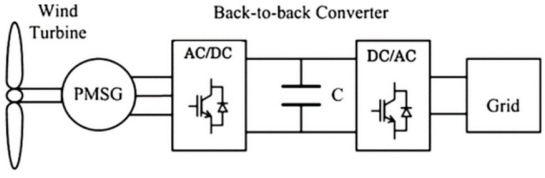

Fig. 1. Block diagram of the variable speed connected grid wind energy system based on PMSG

Consequently, the PMSG has better performance and higher efficiency as compared to other wind turbine generators since the rotor losses contribute to about 20-30% of total generator losses [17]. Even though the PMSG is a synchronous machine, its contribution to the grid inertia is little compared to that of the conventional synchronous generators. This is due to the power electronic based converters through which it is interfaced with the grid as shown in Figure 1 [9].

The purpose of the power electronics based back-back converter equipment is to control the generator rotor angle and convert the electrical power available at the shaft of the generator into high quality power to be integrated to the power grid. The total power generated by the wind turbine is represented in (1) with λ defined in (2) [18]:

$$P = \frac{1}{2}\rho A C_p(\lambda) v^3 \quad (1)$$

$$\lambda = \frac{Rn\pi}{30v} \quad (2)$$

where P is the active power generated by the turbine, ρ is the air density, A is the swept area of the turbine blades, C_p is the power coefficient, λ is the tip speed ratio, v is the wind speed, and n is the generator rotor speed. Since there is no gearbox in the PMSG, the aerodynamic torque (N/m) is equal to the mechanical torque [19] transferred to the generating unit as represented in (3):

$$T_m = \frac{P}{\omega} \quad (3)$$

The modified IEEE 14-bus system with the integration of the PMSG module is shown in Figure 3. The generator is connected to the entire grid via a fully-scaled back to back voltage source power converter (AC/DC/AC). Equations (4) and (5) are the state equations, (6) is the electrical equation, and (7) is the mechanical equation of the PMSG.

$$\frac{di_d}{dt} = \frac{1}{L_d + L_l}(-R_s i_d + w_e.(L_q + L_l).i_q + V_d) \quad (4)$$

$$\frac{di_q}{dt} = \frac{1}{L_q + L_l}(-R_s i_q - w_e[(L_d + L_l)i_d + \psi_f] + V_q) \quad (5)$$

$$w_e = p w_g \quad (6)$$

$$\tau_e = 1.5p((L_d - L_l)i_d i_q + i_q \psi_f) \quad (7)$$

where d and q subscripts represent the physical quantities transformed to the d-q reference frame. R_s is the stator resistance (Ω), L_d and L_q are d and q-axis inductances (H), L_d is the leakage inductance, ψ_f is the permanent magnetic flux (Weber), V_d and $V_q$are d and q-axis voltages, $w_e$is the electro-magnetic speed of the generator (rad/s) and p is the number of pole pairs. Figures 2 and 4 illustrate respectively the d and q-axis equivalent circuits of the PMSG.

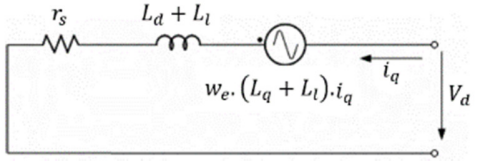

Fig. 2. d-axis equivalent circuit

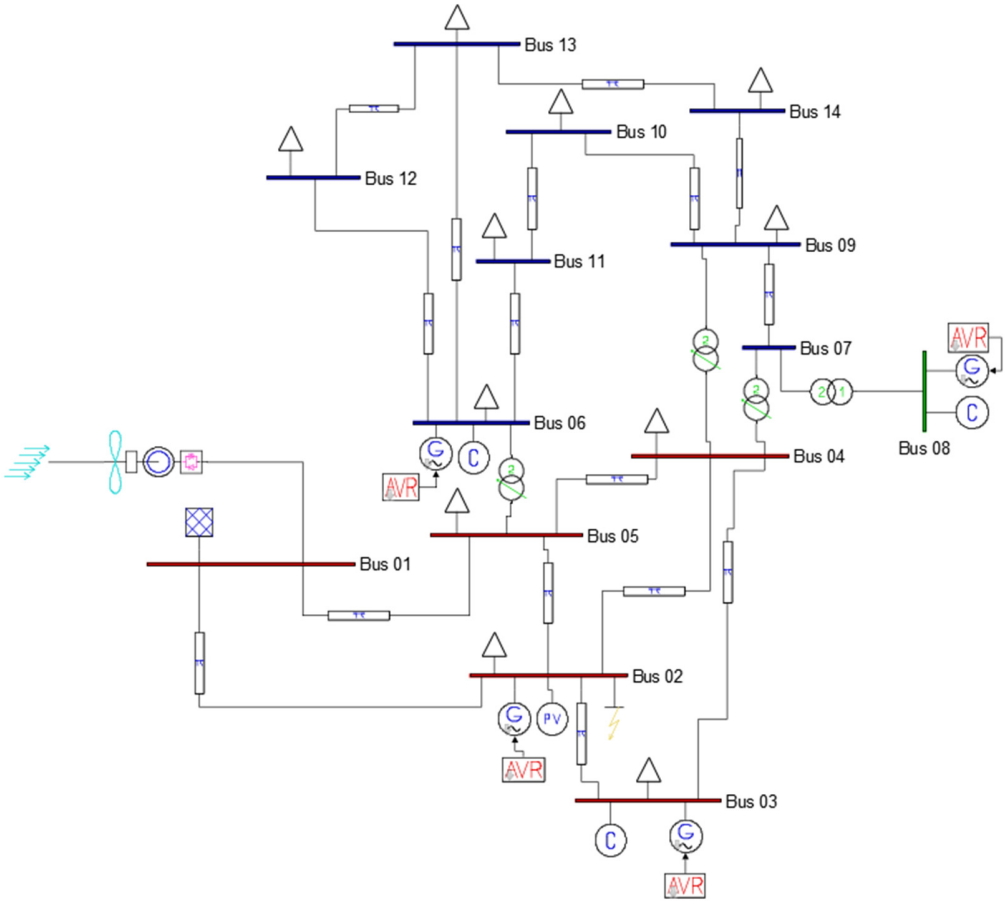

Fig. 3. Modified IEEE-14 bus test system integrated with PMSG-based wind turbine at bus 1

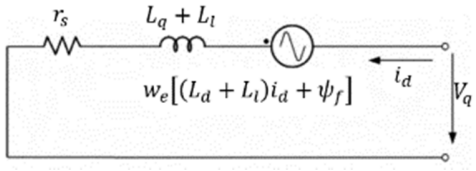

Fig. 4. q-axis equivalent circuit

C. Modeling of the FACTS Devices

Three FACTS devices were employed one from each of the three generations of FACTS [20]. Generally, FACTS devices have a unique feature of rapidly controlling the system by their reactive power management [18, 21]. This characteristic was exploited for the system's TS improvement. Just like the wind generator, the simulation models of the thyristor controlled series capacitor (TCSC), unified power flow controller (UPFC) and the static synchronous compensator (STATCOM) were utilized. TCSC is an important FACTS device which is connected in series in the power system [3]. The total reactance of the TCSC (represented by X_{TCSC}) is given in (8) with W_e and α representing the electrical angular frequency and the firing angle of the thyristor. The TCSC basically improves the power system's TS by adjusting the transmission line impedance:

$$X_{TCSC} = \frac{1}{-W_e C_e + \frac{2\pi - 2\alpha + \sin(2\alpha)}{W_e L \pi}} \quad (8)$$

The makeup of a UPFC combines characteristics of static synchronous compensator together with static series compensator. It simultaneously acts as a shunt and phase shifting device [22]. STATCOM is a voltage source based converter and a shunt connected device. It controls the bus voltage at the place where it is connected [18, 23, 24]. Voltage stability index tool was used to analyze the weakness of the buses in the IEEE-14 bus test system for proper placement of the FACTS devices. The use of voltage stability index creates awareness of the closeness of a power system to voltage collapse or voltage instability [25-26]. Using Figure 5 as an example of the power system's line model (e.g. from bus a to bus b), the fast voltage stability index (FVSI) of any line in the IEEE-14 bus test system is calculated using (9):

$$FVSI_{ab} = \frac{4Z^2 Q_b}{V_a^2 X} \quad (9)$$

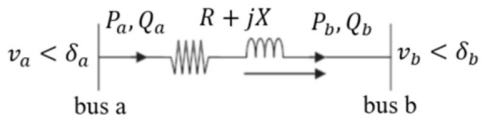

Fig. 5. Power system line model

In (9), Z and X are the line impedance and reactance, V_a and Q_b are the sending end voltage and receiving end reactive power respectively. The closest line to 1 is considered the weakest of all the lines in the system. From the FVSI calculation, line 3 which is found between bus 2 and 3 was identified as the weakest and hence appropriate for integration of FACTS devices. Figure 6 illustrates a plot of the FVSI of all the 20 transmission lines in the system with line 3 indicating the highest value of FVSI aside line 9 (transformer). This means that, more reactive power will be injected through line 3 in each case in order to boost the voltage level and hence improve the TS of the whole system. The modified IEEE-14 bus test system with the integrated PMSG-based wind turbine (at bus 1) and TCSC (between bus 2 and 3) is shown in Figure 7.

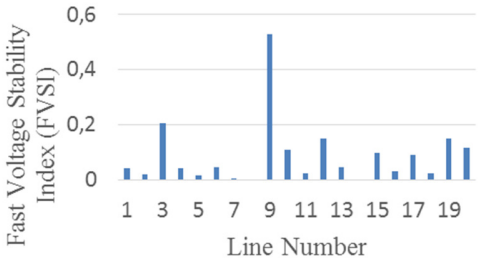

Fig. 6. A bar chat of the Fast Voltage Stability Index of the various lines

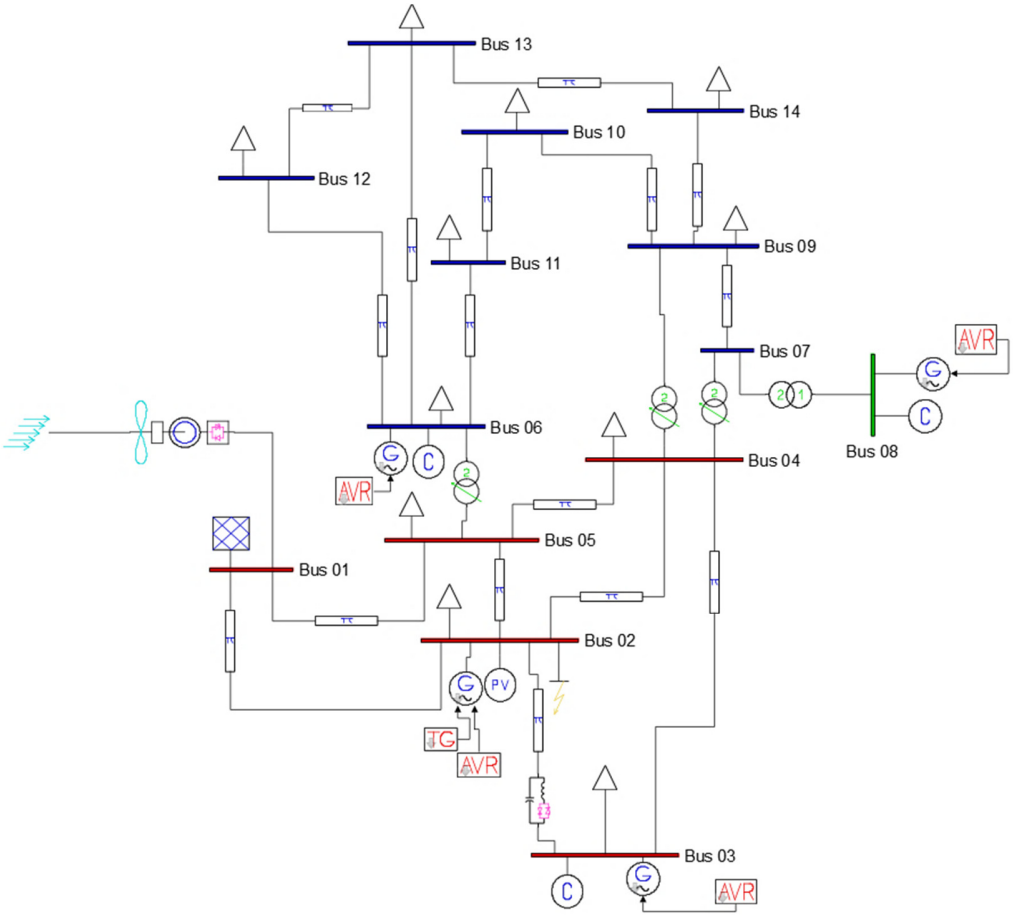

Fig. 7. Modified IEEE-14 bus test system integrated with PMSG-based wine turbine and TCSC

III. SIMULATION RESULTS AND DISCUSSION

Simulations were carried out for four different cases during a three phase to ground fault created in bus 2, in order to compare the transient response of all the systems. The four different cases were:

- Power system integrated with PMSG-based wind turbine
- Power system integrated with wind turbine and TCSC
- Power system integrated with wind turbine and UPFC
- Power system integrated with wind turbine and STATCOM

The fault was created in bus 2 and was set to clear automatically by the system after some time. The fault clearing time varied until the system lost synchronism. The time immediately after the system lost its synchronism was noted and stated as the critical clearing time in each of the above systems. All the synchronous generators in the system were monitored and the critical clearing time in each case was noted with emphasis laid on the generator that was closer to the position of the three phase fault.

A. Case 1: Power System Integrated with PMSG-based Wind Turbine Only

Figures 8-11 illustrate the time domain response of the speed and angle for the synchronous generator 1 (G1) when the fault clearing time is at 2.319s and 2.320s.

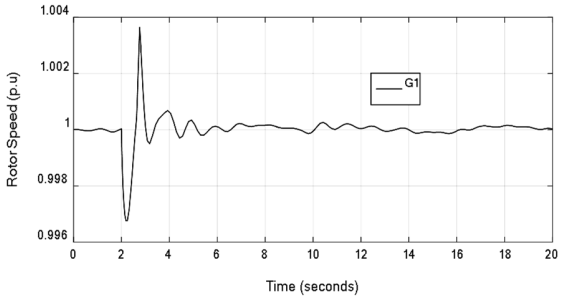

Fig. 8. Rotor speed of G1 at 2.319s fault clearing time

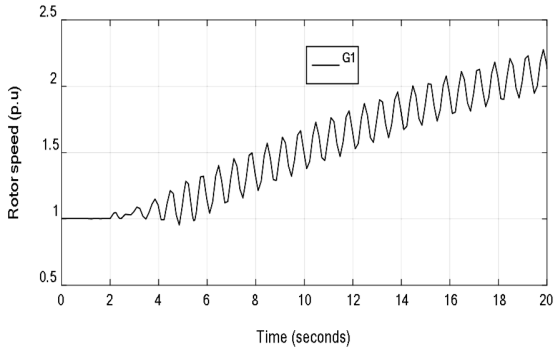

Fig. 9. Rotor speed of G1 at 2.320s fault clearing time

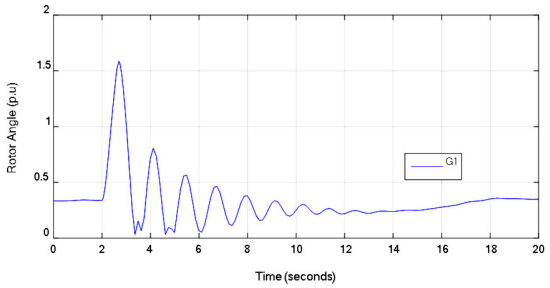

Fig. 10. Rotor angle of G1 at 2.319s fault clearing time

From the swings of both rotor angle and speed deviation, it is discovered that the G1 remains stable when the fault is cleared at or before 0.319s (Figures 8, 10) following the occurrence of the fault. On the other hand, delaying the fault by 0.320s after its occurrence causes the system to lose synchronism (Figures 9, 11). Thus, the speed of the synchronous generator deviates and continues to increase without returning to its original value. In this system, the maximum clearing time for which the synchronous generator remains in synchronism is 2.319s. Beyond this time, the system is unstable. Therefore the CCT of the system integrated with only PMSG-based wind turbine without any FACTS device is 0.319s after the fault.

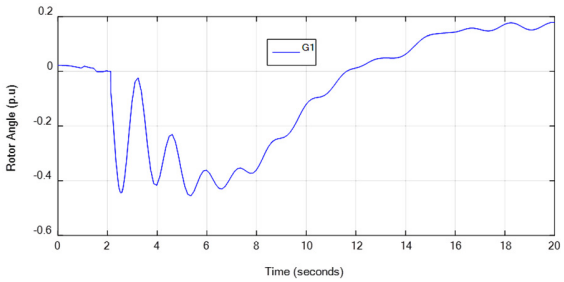

Fig. 11. Rotor angle of G1 at 2.320s fault clearing time

B. Case 2: System Integrated with Wind Turbine and TCSC

Figures 12 and 14 describe the time domain simulation (TDS) results of both rotor speed and angle for the G1 when the fault is cleared at 2.540s whereas Figures 13 and 15 show rotor speed and angle with clearing time of 2.541s. The simulation results of this system show that G1 remains stable with fault clearing time at 2.540s.

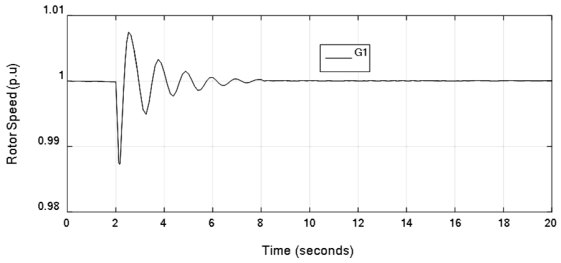

Fig. 12. Rotor speed of G1 at 2.540s fault clearing time

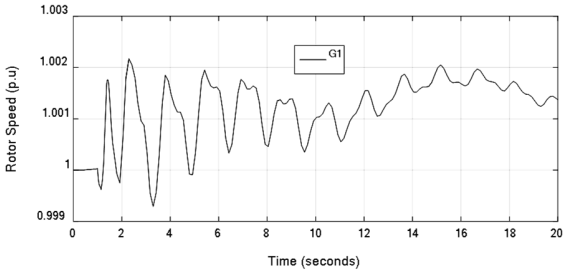

Fig. 13. Rotor speed of G1 at 2.541s fault clearing time

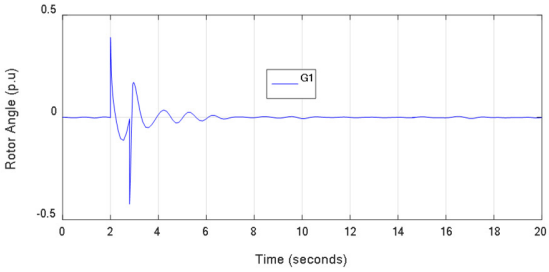

Fig. 14. Rotor angle of G1 at 2.540s fault clearing time

However, delaying fault clearing time to 2.541s makes the system unstable. In other words, clearing the fault at 2.541s instead of 2.540 makes G1 lose synchronism with respect to other synchronous generators in the system. In this case, the CCT of the system is 0.540s following the fault.

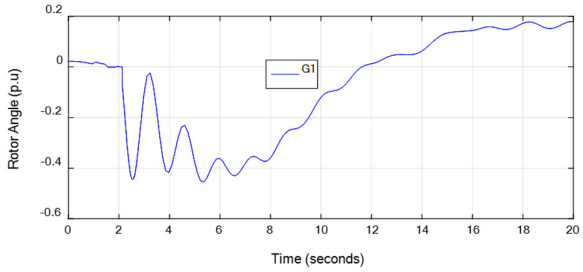

Fig. 15. Rotor angle of G1 at 2.541s fault clearing time

C. Case 3: System Integrated Wind Turbine and UPFC

Figures 16 to 19 show the simulation results for both rotor angles and speed deviations when the fault is cleared at 2.435s and 2.436s. The results show that, clearing the fault before or at 2.435s makes G1 not to lose synchronism (Figures 16, 18) but delaying the fault clearing time to 2.436s causes G1 to lose synchronism (Figure 17, 19). This indicates that the CCT of this system is 0.435s following the occurrence of the three phase fault.

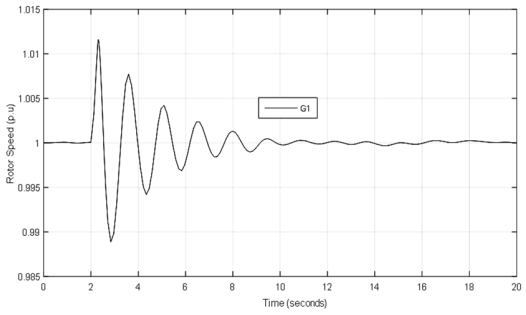

Fig. 16. Rotor speed of G1 at 2.435s fault clearing time

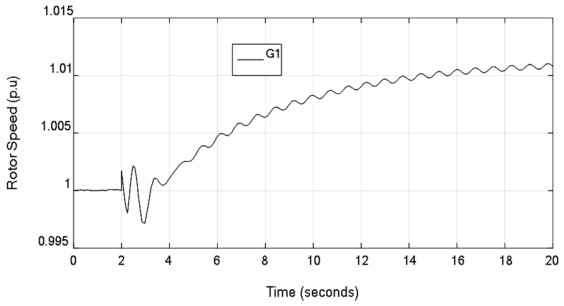

Fig. 17. Rotor speed of G1 at 2.436s fault clearing time

D. Case 4: System Integrated with Wind Turbine and STATCOM

Figures 20-23 illustrate the time domain response of the speed and angle of G1 when the fault clearing time is 2.416s and 2.417s.

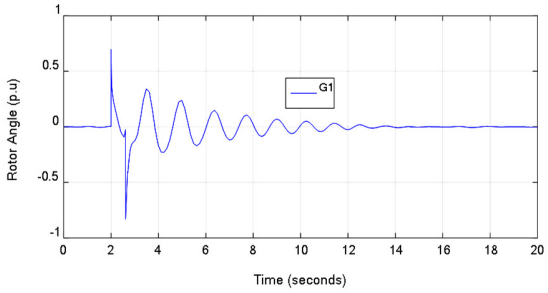

Fig. 18. Rotor angle of G1 at 2.435s fault clearing time

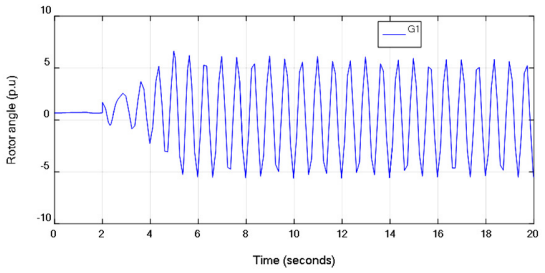

Fig. 19. Rotor angle of G1 at 2.436s fault clearing time

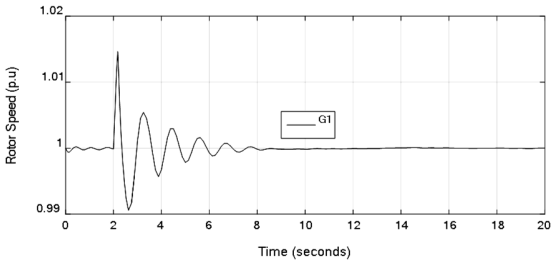

Fig. 20. Rotor speed of G1 at 2.416s fault clearing time

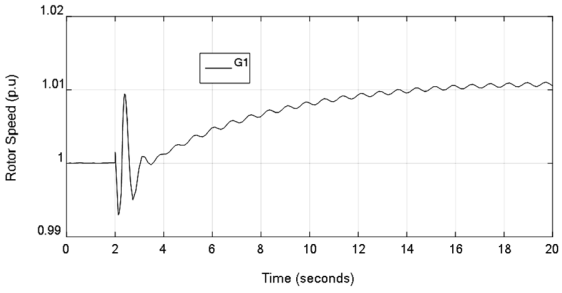

Fig. 21. Rotor speed of G1 at 2.417s fault clearing time

At fault clearing time of 2.416s, G1 regains synchronism just as shown in Figures 23 and 25 for rotor speed and angle respectively. With fault clearing time delayed to 2.417s the G1 does not regain synchronism, making the system unstable as shown in Figures 24 and 26 for speed deviation and rotor angle respectively. Therefore, in this system, clearing the fault at 0.417s instead of 0.416s after the occurrence makes the system totally unstable. Hence, the CCT is 0.416s.

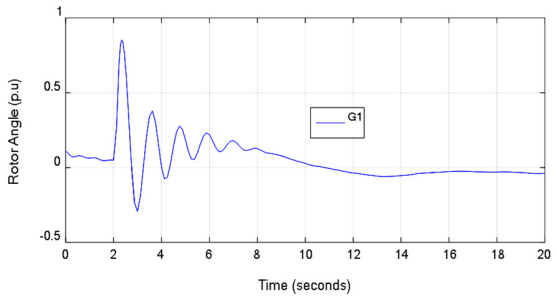

Fig. 22. Rotor angle of G1 at 2.416s fault clearing time

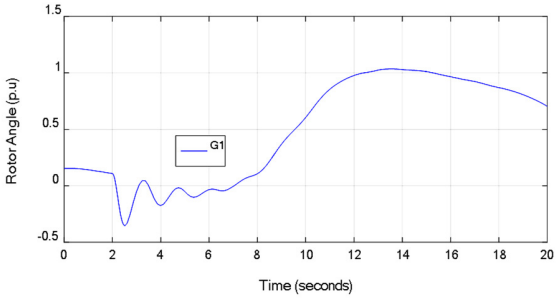

Fig. 23. Rotor angle of G1 at 2.417s fault clearing time

IV. CCT EVALUATION AND IMPROVEMENT

It was concluded from the simulation results that CCT differs from one system to another for all FACTS devices. A summary of the CCT for each case is provided in Table II. The three phase fault was created at bus 2 and at 2s.

TABLE II. SYSTEM CCT SUMMARY

Cases	FCT (stable)	FCT (unstable)	CCT
Case1 (PMSG only)	2.320s	2.319s	0.319s
Case2 (PMSG and TCSC)	2.540s	2.541s	0.540s
Case3 (PMSG and UPFC)	2.4435s	2.436s	0.435s
Case4 (PMSG and STATCOM)	2.416s	2.417s	0.416s

It can be noted that the system with PMSG and TCSC has the longest CCT. In order to visualize clearly the individual contributions of the FACTS devices to the TS improvement in terms of CCT, the CCT of the PMSG-based system is subtracted from the CCT of the systems connected with each of the FACTS devices as shown in (10):

$$CCT\ (improvement)_a = CCT_n - CCT_{PMSG} \qquad (10)$$

where subscript *a* represents TCSC, UPFC or STATCOM. Subscript *n* represents the individual cases (case 1, 2 or 3). This means that, the CCT of the system with the wind turbine only (case 1) which is 0.319s was subtracted from 0.540s, 0.435ss and 0.416s for systems with TCSC, UPFC and STATCOM respectively. The results are summarized in Table III in descending order of improvement.

These results indicate that TCSC has the longest CCT among the three FACTS devices. Therefore, TCSC improves a system integrated with wind turbine better than UPFC and STATCOM. It is also observed that STATCOM has the shortest CCT, so is the weakest FACTS device regarding the TS improvement of the power system. This is in agreement with the findings in [15] for a larger power system.

TABLE III. FACTS DEVICES CONTRIBUTION THE CCT IMPROVEMENT

FACTS devices	CCT	CCT(improvement)
TCSC	0.540s	0.221s
UPFC	0.435s	0.116s
STATCOM	0.416s	0.097s

V. CONCLUSION

This paper aimed at studying the transient stability improvement of a power system connected to a large scale wind turbine using FACTS devices based on the critical clearing time index. Three FACTS devices were considered and each of them was connected individually to investigate their respective contributions to the CCT improvement. In each case, the CCT was stated and the improvement time was identified. This study showed that all the three FACTS devices have different critical clearing times. Thus, they improve the system TS to different extents. It was also discovered that the best FACTS device for TS improvement is TCSC while STATCOM is the weakest FACTS device for transient stability improvement.

ACKNOWLEDGMENT

The authors of this paper wish to thank the Pan African University Institute for Basic Sciences, Technology and Innovation (PAUISTI) for the financial support towards the completion of this work.

REFERENCES

[1] M. K. Nigam, S. Singh, C. Francis, "Effects on power system stability due to integration of distributed generation", Journal of Science and Engineering Education, Vol. 2, pp. 56–60, 2017

[2] N. W. Miller, M. Shao, S. Pajic, R. D. Aquila, Western wind and solar integration study phase 3: Frequency response and transient stability, National Renewable Energy Laboratory, 2014

[3] A. D. Patel, "A review on FACTS devices for the improvement of transient stability", Global Journal of Engineering Science and Resources, Vol. 2, No. 12, pp. 85–89, 2015.

[4] M. L. Tuballa, M. L. S. Abundo, "Operational impact of RES penetration on a remote diesel-powered system in west Papua, Indonesia", Engineering, Technology & Applied Science Research, Vol. 8, No. 3, pp. 2963–2968, 2018

[5] A. Safaei, S. H. Hosseinian, H. A. Abyaneh, "Enhancing the HVRT and LVRT capabilities of DFIG-based wind turbine in an islanded microgrid", Engineering, Technology & Applied Science Research, Vol. 7, No. 6, pp. 2118–2123, 2017

[6] P. Badoni, S. B. Prakash, "Modeling and Simulation of 2 MW PMSG wind energy conversion systems", IOSR Journal of Electrical and Electronics Engineering, Vol. 9, No. 4, pp. 53–58, 2014

[7] Z. Liu, C. Liu, G. Li, Y. Liu, Y. Liu, "Impact study of PMSG-based wind power penetration on power system transient stability using EEAC theory", Energies, Vol. 8, No. 12, pp. 13419–13441, 2015

[8] Z. Tasneem, M. R. I. Sheikh, "Transient stability improvement of a fixed speed wind driven power systemusing permanent magnet synchronous generator", Procedia Engineering, Vol. 90, pp. 698–703, 2014

[9] M. N. I. Sarkar, L. G. Meegahapola, M. Datta, "Reactive power management in renewable rich power grids: A review of grid-codes, renewable generators, support devices, control strategies and optimization algorithms", IEEE Access, Vol. 6, pp. 41458–41489, 2018

[10] R. K. Tiwari, K. K. Sharma, "Simulation and modeling of wind turbine using PMSG", International Journal of Recent Research and Review, Vol. 7, No. 2, pp. 46–50, 2014

[11] P. Shen, L. Guan, Z. Huang, L. Wu, Z. Jiang, "Active-current control of large-scale wind turbines for power system transient stability improvement", Energies, Vol. 11, Article ID 1995, 2018

[12] D. Kalpaktsoglou, S. Pouros, K. Kleidis, "Improving the efficiency of a wind turbine using thyristor switched series capacitors: A simulation study", WSEAS Transactions on Power Systems, Vol. 14, pp. 33–38, 2019

[13] A. A. Hussein, M. H. Ali, "Comparison among series compensators for transient stability enhancement of doubly fed induction generator based variable speed wind turbines", IET Renewable Power Generation, Vol. 10, No. 1, pp. 116–126, 2016

[14] M. Amroune, T. Bouktir, "Power system transient stability analysis with high wind power penetration", International Electrical Engineering Journal, Vol. 4, No. 1, pp. 907–913, 2013

[15] P. A. Aysha, A. Baby, "Transient stability assessment and enhancement in power system", International Journal of Modern Engineering Research, Vol. 4, No. 9, pp. 61–65, 2014

[16] M. A. Pai, Energy function analysis for power system stability, Kluwers Academic Publishers, 1989

[17] A. Rolan, A. Luna, G. Vazquez, D. Aguilar, G. Azevedo, "Modeling of a variable speed wind turbine with a permanent magnet synchronous generator", IEEE International Symposium on Industrial Electronics, Seoul, South Korea, July 5-8, 2009

[18] R. Jadeja, S. Patel, S. Chauhan, "STATCOM: A preface to power quality in power systems performance", Engineering, Technology & Applied Science Research, Vol. 6, No. 1, pp. 895–905, 2016

[19] M. A. Husain, A. Tariq, "Modeling and study of a standalone PMSG wind generation system using MATLAB/SIMULINK", Universal Journal of Electrical and Electronic Engineering, Vol. 2, No. 7, pp. 270–277, 2014

[20] B. T. R. Rao, P. Chanti, N. Lavanya, S. C. Sekhar, Y. M. Kumar, "Power system stability enhancement using fact devices", International Journal of Engineering Research and Applications, Vol. 4, No. 4, pp. 339–344, 2014

[21] M. Y. A. Khan, U. Khalil, H. Khan, A. Uddin, S. Ahmed, "Power flow control by unified power flow controller", Engineering, Technology & Applied Science Research, Vol. 9, No. 2, pp. 3900–3904, 2019

[22] R. Chavan, R. S. Lodhi, "Selection of FACTs devices for better reactive power compensation through capacitor", International Journal of Engineering and Techniques, Vol. 2, No. 5, pp. 28–35, 2016

[23] A. S. Yome, N. Mithulananthan, K. Y. Lee, "Static voltage stability margin enhancement using STATCOM, TCSC and SSSC", IEEE/PES Transmission & Distribution Conference & Exposition: Asia and Pacific, Dalian, China, August 18, 2005

[24] K. G. Damor, D. M. Patel, V. Agrawal, H. G. Patel, "Comparison of different fact devices", International Journal of Science Technology & Engineering, Vol. 1, No. 1, pp. 12-17, 2014

[25] A. S. Telang, P. P. Bedekar, "Application of voltage stability indices for proper placement of STATCOM under load increase scenario", International Journal of Energy and Power Engineering, Vol. 10, No. 7, pp. 998–1003, 2016

[26] I. A. Samuel, A new voltage stability index for predicting voltage collapse in electrial power system networks, Covenant University, 2017